

# Picosecond Fluorescence Spectroscopy on Excimer Formation and Excitation Energy Transfer of Pyrene In Langmuir-Blodgett Monolayer Films

Iwao Yamazaki,\* Naoto Tamai, and Tomoko Yamazaki

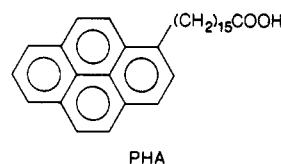
Institute for Molecular Science, Myodaiji, Okazaki 444, Japan (Received: December 3, 1986)

Molecular association of pyrene chromophores has been studied with Langmuir-Blodgett (LB) monolayer films consisting of stearic acid and small amounts of 16-(1-pyrenyl)hexadecanoic acid. Picosecond time-resolved fluorescence spectra have shown four fluorescence bands originating from (1) a ground-state dimer (band D with vibrational peaks at 381, 401, and 422 nm), (2) a monomer (band M with vibrational peaks at 377, 397, and 421 nm), (3) an excimer (a structureless band  $E_1$  with a peak at 420 nm), and (4) another type of excimer (a structureless band  $E_2$  with a peak at 470 nm).  $E_2$  was assigned as a fluorescence from a two-center, sandwich-type excimer which corresponds to the well-known pyrene excimer in solution, while  $E_1$  was assigned as a fluorescence from a one-center type excimer. In the initial time region (0-200 ps), the D band is dominant, and its decay is associated with a rise of the  $E_2$  band. The excimer band  $E_1$  forms much faster than band  $E_2$ . The fluorescence decay curves of the isolated monomer (band M) are interpreted in terms of two-dimensional energy transfer and trapping, leading to the conclusion that the LB monolayer film exhibits an island structure, i.e., a nonuniform distribution of guest molecules.

## Introduction

A Langmuir-Blodgett (LB) film is a mono- or multilayered molecular assembly which is prepared by transferring a compressed monolayer spread on a water surface onto a substrate.<sup>1</sup> In the LB film, one can expect to observe new aspects of photochemical and photophysical processes of electronically excited molecules, because a uniform thin monolayer or its multilayers with the two- or three-dimensional order might show configurational and dynamical behaviors quite different from those of a homogeneous solution or from the bulk properties of crystals. Recent studies in polymer photophysics have shown that restricted motion of aromatic chromophores linked by a hydrocarbon chain yields several kinds of excimer or exciplex with different conformations depending on the conformational and configurational properties of the polymer chains.<sup>2-5</sup> In other examples of aromatic molecules adsorbed on the surfaces of silica gel<sup>6-10</sup> and zeolite,<sup>11</sup> it has been shown that pyrene molecules within pores in the surface form a ground-state dimer and that the excimer formation which occurs through the dimer is much faster than that in solution where excimer formation is a diffusion-controlled encounter process.<sup>12</sup>

Recently, we have examined the molecular association of pyrene chromophores in a LB film consisting of stearic acid and 16-(1-pyrenyl)hexadecanoic acid (PHA) with a picosecond time-resolved fluorescence spectrophotometer.<sup>13</sup> It was found that pyrene



chromophores in the LB film form a ground-state dimer. This dimer formation might be analogous to those observed in silica gel<sup>6-10</sup> and zeolite<sup>11</sup> surfaces and in a cyclohexane matrix at 77 K.<sup>14</sup> Note that, in the initial procedure of LB film preparation, a stearic acid monolayer including a small amount of PHA is spread on the water surface and compressed. Then, in a certain fraction of PHA molecules added, two or more PHA molecules assemble to form pyrene aggregates which are surrounded by a number of stearic acid molecules. A pair of pyrene chromophores within a cage of stearic acid molecules might be forced to form a metastable ground-state dimer, if the pyrene molecules in the ground state are repulsive to each other, as is expected from a spectroscopic analysis of the parallel conformation.<sup>13</sup> Otherwise, it has been demonstrated that a pair of pyrene molecules in the ground state are attractive in other than a parallel conformation.<sup>3</sup> The ratio of the number density of isolated monomers to that of dimers and/or higher aggregates should depend on the concentration of PHA. The fluorescence decay curves of the LB film appear to be very complicated probably because various emitting species or sites of pyrene chromophores exist in the LB film.

The present paper reports further detailed analysis of the time-resolved fluorescence spectra and the fluorescence decay curves of pyrene chromophores in a LB film. The fluorescence decay curves are interpreted in terms of (1) a rapid process of excimer formation through the ground-state dimer and (2) slower decays of the isolated monomer of the pyrene chromophore, which can be analyzed in terms of two-dimensional energy transfer and trapping.

## Experimental Section

**Preparation of LB Films.** PHA was purchased from Molecular Probe Co., U.S.A. Stearic acid, G.R. grade, obtained from Wako Pure Chemical Co., Osaka, was purified five times by recrystallization from an alcohol solution.

A mixture of stearic acid and PHA was spread from a Benzene solution ( $3.0 \times 10^{-3}$  M) onto the water surface in a Langmuir trough (Joyce-Loeble Trough 4). The concentration of PHA was

(1) Kuhn, H.; Möbius, D.; Bücher, H. In *Techniques of Chemistry*, Weissberger, A., Rossiter, B. W., Eds.; Wiley: New York, 1972; Vol. 1, Part 3B, pp 577-702.

(2) Zachariasse, K. A.; Duveneck, G.; Kuhnle, W. *Chem. Phys. Lett.* **1985**, *113*, 337.

(3) (a) De Schryver, F. C.; Moens, L.; Van der Auwerer, M.; Boens, N.; Monnerie, L.; Bokobza, L. *Macromolecules* **1982**, *15*, 64. (b) De Schryver, F. C.; Vandendriessche, J.; Toppet, S.; Demeyer, K.; Boens, N. *Macromolecules* **1982**, *15*, 406. (c) Collart, P.; Toppet, S.; Zhou, Q. F.; De Schryver, F. C. *Macromolecules* **1985**, *18*, 1026.

(4) Winnik, M. A., Ed. *Photophysical and Photochemical Tools in Polymer Science*, NATO Advanced Study Institute Series; Reidel: Dordrecht, 1986; Vol. 182.

(5) Turro, N. J.; Kuo, P. L. *Langmuir* **1986**, *2*, 438.

(6) Hara, K.; de Mayo, P.; Ware, W. R.; Weedon, A. C.; Wong, G. S. K.; Wu, K. C. *Chem. Phys. Lett.* **1980**, *69*, 105.

(7) Bauer, R. K.; Borenstein, R.; de Mayo, P.; Okada, K.; Rafalska, M.; Ware, W. R.; Wu, K. C. *J. Am. Chem. Soc.* **1982**, *104*, 4635.

(8) Bauer, R. K.; de Mayo, P.; Okada, K.; Ware, W. R.; Wu, K. C. *J. Phys. Chem.* **1983**, *87*, 460.

(9) Avnir, D.; Busse, R.; Ottolenghi, M.; Wellner, E.; Zachariasse, K. A. *J. Phys. Chem.* **1985**, *89*, 3521.

(10) Wellner, E.; Ottolenghi, M.; Avnir, D.; Huppert, D. *Langmuir* **1986**, *2*, 616.

(11) Suib, S. L.; Kostapapas, A. *J. Am. Chem. Soc.* **1984**, *106*, 7705.

(12) Birks, J. B. *Photophysics of Aromatic Molecules*; Wiley-Interscience: New York, 1970.

(13) Yamazaki, T.; Tamai, N.; Yamazaki, I. *Chem. Phys. Lett.* **1986**, *124*, 326.

(14) Mataga, N.; Torihashi, Y.; Ota, Y. *Chem. Phys. Lett.* **1967**, *1*, 385.

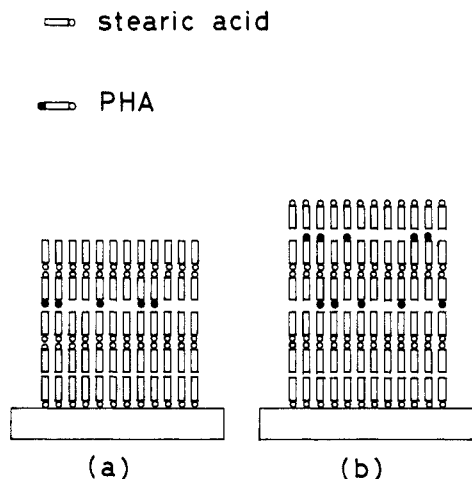


**Figure 1.** Schematic illustration of the multilayer structure of the LB films used in this study. Solid circles represent the pyrene chromophores of PHA, open circles the carboxyl group, and rods the hydrocarbon chain.

changed from 0.7 to 26 mol %. The surface pressure–area isotherms of the mixed monolayer including PHA exhibited a steep increase in the surface pressure, indicating formation of a compressed monolayer with a limiting area of  $0.21\text{--}0.23\text{ nm}^2$ .<sup>13</sup> Under the subphase conditions of pH 6.7 and  $20^\circ\text{C}$ , two layers of Y-type were transferred onto a quartz substrate at  $25\text{ mN m}^{-1}$  and at a transfer rate of  $20\text{ mm/min}$ . The quartz substrates used here were precoated with five layers of cadmium stearate so as to minimize any influence of the quartz surface on the kinetics of the photophysical processes. The LB films in this study were prepared by following the procedure of Nakahara<sup>15</sup> and also those of Sugi.<sup>16</sup>

The structures of the LB films used here are illustrated schematically in Figure 1. Seven or eight layers were deposited on a quartz plate in the following order: (1) five layers of the calcium salt of stearic acid, (2) a monolayer or bilayer consisting of stearic acid and small amounts of PHA, and (3) a monolayer of stearic acid. An outer layer of stearic acid prevented the multilayered structure from being destroyed. The concentration of PHA was changed from 0.7 to 26 mol %.

**Apparatus.** Time-resolved fluorescence spectra and fluorescence decay curves were measured with a picosecond time-resolved emission spectrophotometer.<sup>17</sup> The picosecond laser system as an excitation source was composed of a synchronously pumped, cavity dumped dye laser (Spectra Physics 375 and 344S) and a mode-locked argon ion laser (Spectra Physics 171-18). The laser was operated with a repetition rate of  $800\text{ kHz}$  and a single-pulse duration of  $6\text{ ps}$  (fwhm). The intensity of the dye laser is  $6.8 \times 10^{-4}\text{ W/cm}^2$  at  $570\text{ nm}$  which corresponds to  $10^8\text{ photons/cm}^2$  per single pulse. The photomultiplier employed here was a proximity-type of microchannel-plate photomultiplier (Hamamatsu R1564U) with two microchannel plates. The electron transit-time spread of this photomultiplier is significantly narrower than that of conventional photomultipliers. As a result, the observed laser pulse width was as short as  $60\text{ ps}$  (fwhm).

**Time-Resolved Fluorescence Spectra.** Fluorescence decay curves were measured for different monitoring wavelengths. The wavelength of the monochromator was driven successfully in a  $0.625\text{-nm}$  step under the control of the computer. Usually, the accumulation time for one decay curve was  $20\text{ s}$ ; thus it took  $2\text{ h}$  to measure the decay curves at  $320\text{ nm}$  monitoring wavelengths ranging from  $350$  to  $550\text{ nm}$ . From a series of decay curves, we obtained the time-resolved spectra with a minimum time difference of  $2.5\text{ ps}$  by plotting the fluorescence intensity at a particular delay time as a function of wavelength. The decay curve measurements

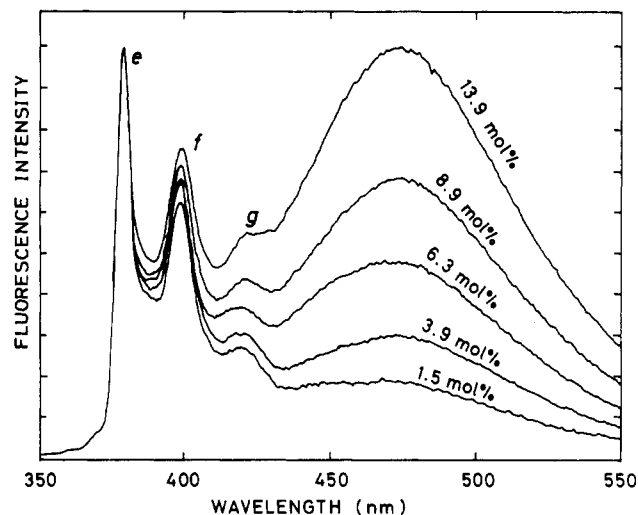


**Figure 2.** Fluorescence spectra of LB monolayer films containing pyrene chromophores at various concentrations. The wavelengths of peak positions are summarized in Table II.

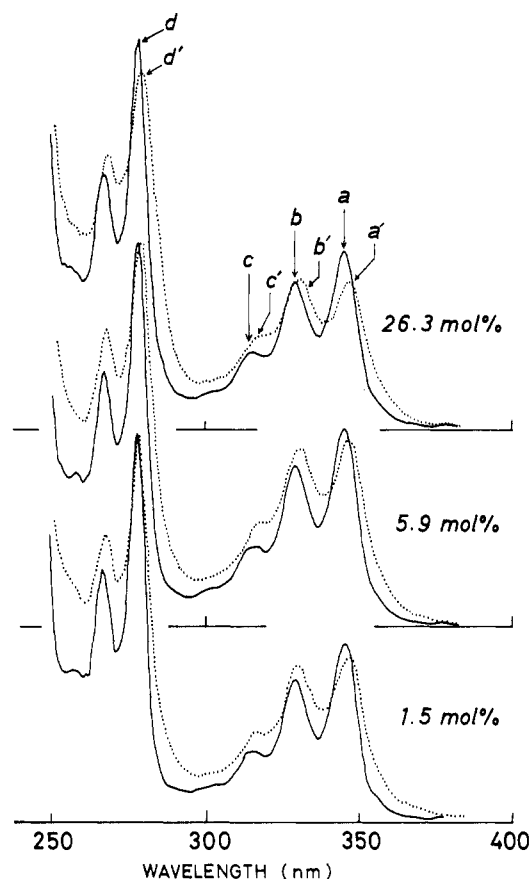


**Figure 3.** Fluorescence excitation spectra of LB films containing pyrene chromophores at various concentrations. The spectra were obtained by monitoring at  $397\text{ nm}$  (—) and  $474\text{ nm}$  (·····) corresponding to monomer and excimer bands, respectively. The wavelengths of peak positions are summarized in Table I.

and the data processing for the time-resolved spectra were made with a computer system.

## Results and Discussion

Fluorescence spectra of the steady excitation are shown in Figure 2 for LB films with various concentrations of PHA. The fluorescence spectrum consists of a structured band of pyrene monomer and a broad structureless band of excimer. The monomer fluorescence band exhibits vibrational bands with maxima at  $377$ ,  $397$ , and  $419\text{ nm}$ , while the excimer spectrum has a peak at  $474\text{ nm}$ . The intensity of the excimer band increases with

(15) Nakahara, H. *J. Oil Chem. Jpn.* **1982**, *31*, 559.

(16) Sugi, M.; Saito, M.; Fukui, T.; Iizima, S. *Solid State Phys. (Kotai Butsuri)* **1982**, *17*, 744.

(17) Yamazaki, I.; Kume, H.; Tamai, N.; Tsuchiya, H.; Oba, K. *Rev. Sci. Instrum.* **1985**, *56*, 1187.

**TABLE I: Band Positions of the Fluorescence Excitation Spectrum and the Absorption Spectrum**

band	excitation spectrum		absorption spectrum	
	monitoring wavelength, nm	band position, nm	concn, mol %	band position, nm
a	397	345.3	3.6	345.5
b		329.2		329.5
c		315.5		315.9
d		277.6		278.3
a'	470	347.2	26.8	347.4
b'		331.1		331.5
c'		317.5		317.3
d'		279.4		283.2

increasing concentration of PHA. Profiles of the fluorescence spectrum and their change with PHA concentration are almost the same as those observed in a fluid solution of pyrene.<sup>12</sup> Contrary to the case of a fluid solution, however, the fluorescence excitation spectrum in the LB film is different according to whether the monomer or the excimer fluorescence is monitored. Figure 3 shows the fluorescence excitation spectra for three PHA concentrations, which were monitored at 397 nm (monomer) and a 474 nm (excimer). The band positions in these spectra are summarized in Table I. It is seen that the excitation spectrum of the excimer is shifted to a longer wavelength compared with that of the monomer; the monomer spectrum for the  $^1L_a$  absorption band exhibits peaks at 345, 329, and 315 nm (referred to as bands a, b, and c, respectively), while the excimer spectrum peaks at 347, 331, and 317 nm (referred to as bands a', b', and c', respectively). The intensity distribution of these vibrational bands is different between the monomer and the excimer spectra. As the PHA concentration is decreased, the excitation spectrum of the excimer resembles closely that of the monomer, indicating that the contributions of bands a', b', and c' become small. The excitation spectra of the monomer and of the excimer respectively correspond well to the absorption spectra of low and high PHA concentrations (Table I). This means that the excimer state forms from a species giving absorption bands a', b', and c', different from the monomer. We assign this species to a loosely coupled molecular pair of pyrene, from which the excimer forms through only a small displacement of the pyrene chromophore.

**Time-Resolved Fluorescence Spectra.** Figure 4 shows the time-resolved fluorescence spectra of LB films with a PHA concentration of 13.9 mol %. Each spectrum is normalized to the maximum intensity and is separated into components. It is seen that the spectrum changes significantly with time on going from the picosecond to the nanosecond time region. Each of the time-resolved spectrum can be analyzed by assuming four spectral components. Then the spectral change can be interpreted as follows. (1) In the short time region, 0–200 ps, a fluorescence band D appears with three peaks at 381, 401, and 422 nm (referred to as bands e', f', and g', respectively). These peaks are shifted by 1–4 nm to the red compared with those of band M that appears in a longer time region. Band D can be regarded as due to a fluorescence transition associated with the absorption band of the dimer, i.e., a', b', and c'. The peak positions are summarized in Table II. Thus band D can be assigned reasonably to fluorescence from the ground-state dimer of pyrene rings. (2) After 1 ns, a broad band E<sub>2</sub> appears with a peak around 470 nm. This band corresponds to the well-known excimer fluorescence band in solution.<sup>11</sup> (3) In the time period of 100 ps–2 ns, the three peaks of D band (e', f', and g') are gradually blue-shifted, and finally the D band is changed into a different band M with peaks at 377, 397, and 421 nm (referred to as e, f, and g). This band is identical with the monomer band in the fluorescence spectrum of stationary excitation (e, f, and g in Figure 2). (4) A component analysis of the time-resolved spectra reveals another band E<sub>1</sub> in the time region of 100 ps–10 ns. We assign the E<sub>1</sub> band as due to another type of excimer whose conformation will be different from that of E<sub>2</sub>.

Spectral profiles in the time-resolved spectra are strongly dependent on the PHA concentration; as the concentration of PHA

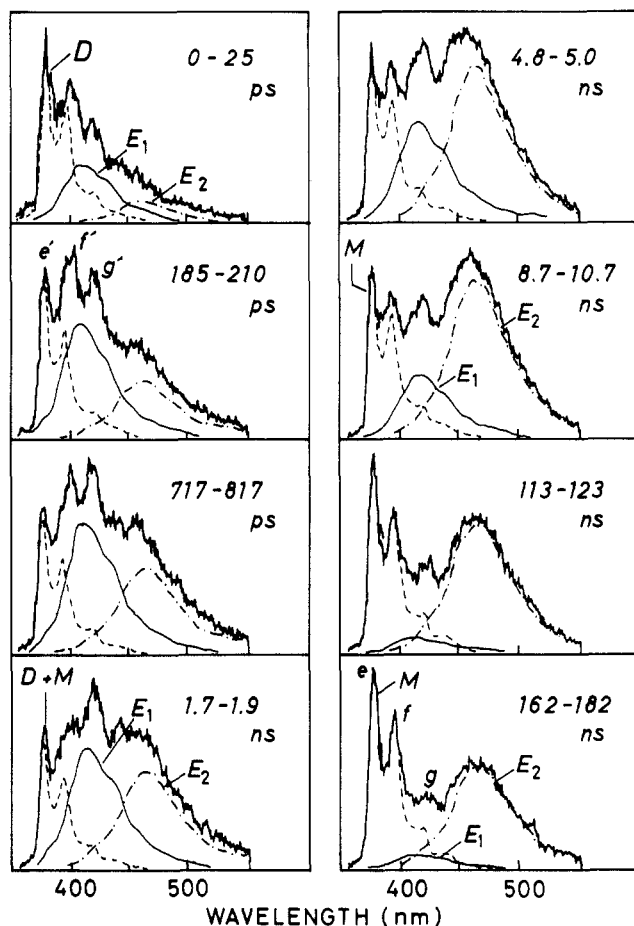


**Figure 4.** Time-resolved fluorescence spectra of a LB monolayer film containing 13.9 mol % pyrene chromophores. The excitation wavelength is 315 nm. The time zero corresponds to the time in which the excitation laser pulse reaches maximum intensity.

**TABLE II: Band Positions in the Fluorescence Spectra**

band	time-resolved fluorescence spectrum		steady fluorescence spectrum	
	time region	band position, nm	concn, mol %	band position, nm
e	after 10 ns	377	3.6	377
f		397		397
g		421		421
excimer E <sub>2</sub>		470		470
e'	0–200 ps	381		
f'		401		
g'		422		
excimer E <sub>1</sub>		420		
excimer E <sub>2</sub>		470		

is lowered, the excimer fluorescences of E<sub>1</sub> and E<sub>2</sub> make only minor contributions. The time-resolved fluorescence spectra of a lower PHA concentration (2.0 mol %) are shown in Figure 5. Both excimer bands, E<sub>1</sub> and E<sub>2</sub>, have only small contributions throughout the whole time region, and also the contribution of the dimer band D is small, as shown below. As has been stated before, the band position of the first vibrational band of D (band e') is shifted to the blue with time (Figure 4). The wavelength of this band position is plotted as a function of time in Figure 6, for three PHA concentrations. It can be seen that, at substantially higher PHA concentrations, the band shift occurs in the time region of 100 ps–100 ns with 13.9 mol % of PHA concentration and in time region 100 ps–10 ns with 28.6 mol %. These shifts should be associated with the transition of the ground-state dimer state (D) to the excimer state (E<sub>2</sub>). On the other hand, at low PHA concentration (0.8 mol %), the band shift is negligibly small, suggesting that only a monomer band M appears in the time-

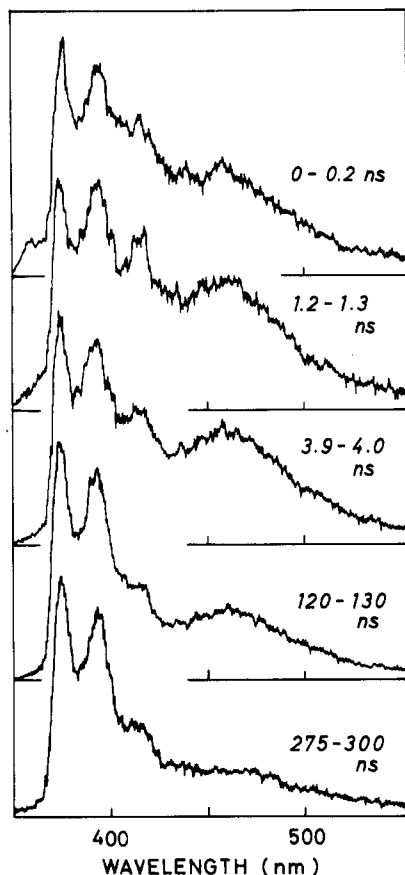


**Figure 5.** Time-resolved fluorescence spectra of a LB film monolayer film containing 2.6 mol % pyrene chromophores. The excitation wavelength is 315 nm. The time zero corresponds to the time in which the excitation laser pulse reaches maximum intensity.

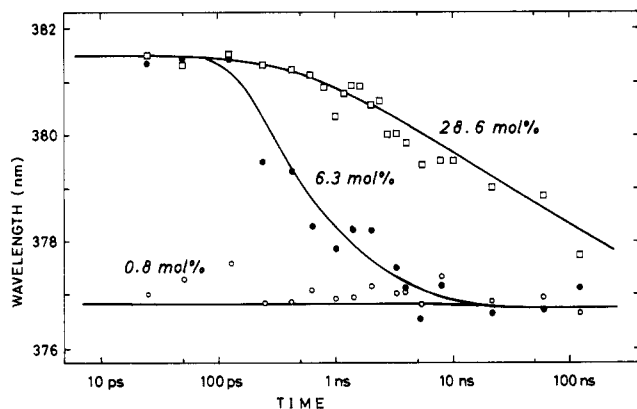


**Figure 6.** Plots of the peak position of the fluorescence bands of the pyrene monomer and dimer in the time-resolved spectrum (Figure 4), as a function of time after pulsed excitation.

resolved spectra throughout the time regions concerned here.

Note that the LB films employed in this study are prepared from compressed monolayers including stearic acid and small amounts of PHA. Thus a pair of pyrene chromophores, which is surrounded by stearic acid molecules within a cage, may be forced to form a metastable ground-state dimer. Thus such a molecular pair might exhibit an absorption band shifted to the red compared to the isolated monomer. The probability that two or more pyrene chromophores are encountered increases with increasing PHA concentration.

With pyrene, formation of a ground-state dimer is known in several cases: pyrene adsorbed on surfaces of silica gel<sup>6-10</sup> and zeolite<sup>11</sup> and pyrene in a cyclohexane matrix at 77 K.<sup>14</sup> Common to these cases, the excitation spectrum of the excimer fluorescence is shifted by 10–20 nm to the red compared to that of the monomer. Furthermore, according to the fluorescence rise and decay

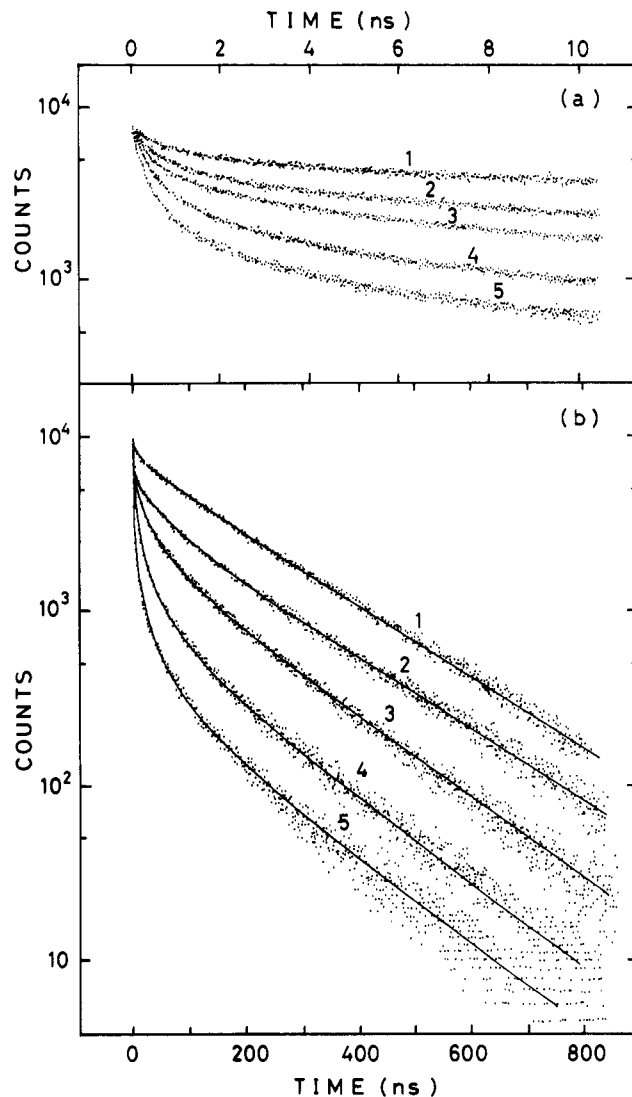


**Figure 7.** Fluorescence decay curves of the LB films, monitored at 377 nm corresponding to the dimer (D) and monomer (M) band regions, for the time regions of 3–10 (a) and 0–800 ns (b). The concentrations of the pyrene chromophores are (1) 0.8, (2) 2.2, (3) 6.5, (4) 14.8, and (5) 28.6 mol %.

curves in these cases, the excimer forms much faster (less than 0.1 ns) than in solution where excimer formation is a diffusion-controlled encounter process.<sup>12</sup> All these behaviors are similar to the present results for a LB film.

**Decay Curves of Fluorescence Bands D and M.** Parts a and b of Figure 7 show the fluorescence decay curves monitored at 377 nm for time scales of 0–10 and 0–800 ns, respectively. The fluorescence decay curve monitored at 377 nm are recognized as a superposition of fluorescence decays of the dimer D and the monomer M. According to the spectrum analysis (Figure 4) and the time course of the fluorescence band shift (Figure 6), it can be seen that the dimer fluorescence band D disappears 10 ns after excitation and that the fluorescence band M becomes dominant after 10 ns. Therefore, the decay curve in the time region of 0–200 ps (Figure 7a) can be recognized as the time behavior of the dimer fluorescence D, while the decay curve after 10 ns (Figure 7b) is of the isolated monomer M. The decay curve in the intermediate time region 200 ps–10 ns is the superposition of the decays of both components.

The fast decay of D which appears in the short time region (Figure 7a) can be attributed to a transition of the ground-state dimer to the excimer state. In order to obtain approximate decay constants of these fast decays, we analyzed the decay curves on the basis of multiexponential decay kinetics. The lifetimes of the fastest decaying component were estimated to be  $170 \pm 10$  ps, irrespective of the PHA concentration. The amplitude of this fast

**TABLE III: Decay Curve Analysis of the Pyrene Monomer Fluorescence (Band M) Monitored at 377 nm<sup>a</sup>**

concn of PHA, mol %	$A_1$	$A_2$	$2\gamma_A$	$n_A, 10^{13} \text{ cm}^{-2}$	
				exptl	calcd
0.8	0.6	0.4	1.9	4.5	0.012
2.2	0.8	0.2	2.3	5.5	0.085
6.7	0.9	0.1	2.5	5.9	0.65
14.8	0.95	0.05	2.9	6.9	2.8
28.6	0.95	0.05	3.0	7.1	4.7

<sup>a</sup> Analysis according to eq 1.

component is changed from 40% to 70% in the concentration range from 6.7 to 28.6 mol %. At concentrations lower than 2 mol %, the contribution of the fast decaying component is negligible.

The fluorescence decay profile after 10 ns (Figure 7b), i.e., the decay curve of the isolated monomer (M), depends strongly on the concentration of PHA. It can be seen in Figure 7b that, in the low concentration limit of PHA, the decay is almost single exponential. On increasing the concentration, however, the decay curve deviates from the exponential form. We analyzed these nonexponential decay curves by using a modified equation for excitation energy transfer and trapping in the two-dimensional molecular arrangement.<sup>18-22</sup>

$$\rho(t) = A_1 \exp[-t/\tau_D - 2\gamma_A(t/\tau_D)^{1/3}] + A_2 \exp(-t/\tau_D) \quad (1)$$

where

$$\gamma_A = (2/3)\pi n_A R_0 \quad (2)$$

Here  $\tau_D$  is the mean lifetime of the donor without acceptor;  $n_A$  is the density of energy traps; and  $R_0$  is the critical transfer distance where the energy transfer and the intrinsic energy deactivation of the excited donor take place with an equal probability. The  $\tau_D$  value was determined to be 215 ns from the single exponential decay of the LB film at the lowest PHA concentration. Curve fitting on the basis of eq 1 was carried out by varying the values of  $\gamma_A$  and  $A_2/A_1$ . The results of the decay curve analysis are summarized in Table III. It is seen that the amplitude of the exponential decay term  $A_2$  is fairly large at lower concentrations of PHA, whereas at concentrations above 14 mol %, it becomes negligibly small. For the two-dimensional energy-transfer kinetics, the original equation of Hauser et al.,<sup>18</sup> i.e., the first term of eq 1, is based on the assumption that acceptor molecules around a donor are distributed uniformly and randomly in a two-dimensional plane. The present result that an additional exponential term, i.e., the second term of eq 1, contributes largely at low concentrations suggest probably an irregular distribution of chromophores on the two-dimensional surface. It can be considered that PHA molecules in the LB film form two types of domains; in one domain pyrene chromophores assemble to form an island structure where the excitation is trapped on nearby aggregated species, but in the other domain they are isolated and the excited pyrene chromophores decay with an intrinsic lifetime. One should note that kinetic equations similar to eq 1 instead of the original equation of Hauser et al.<sup>18</sup> were generally used in recent studies on fluorescence quenching for dye molecules adsorbed on semiconductors or insulators.<sup>19-22</sup>

The decay curve analysis of the pyrene monomer shows that the excited pyrene chromophores in LB films undergoes fluorescence quenching. It is reasonably assumed that excitation energy trapping occurs at aggregated species of pyrene chromophores. The number density of energy traps can be evaluated from

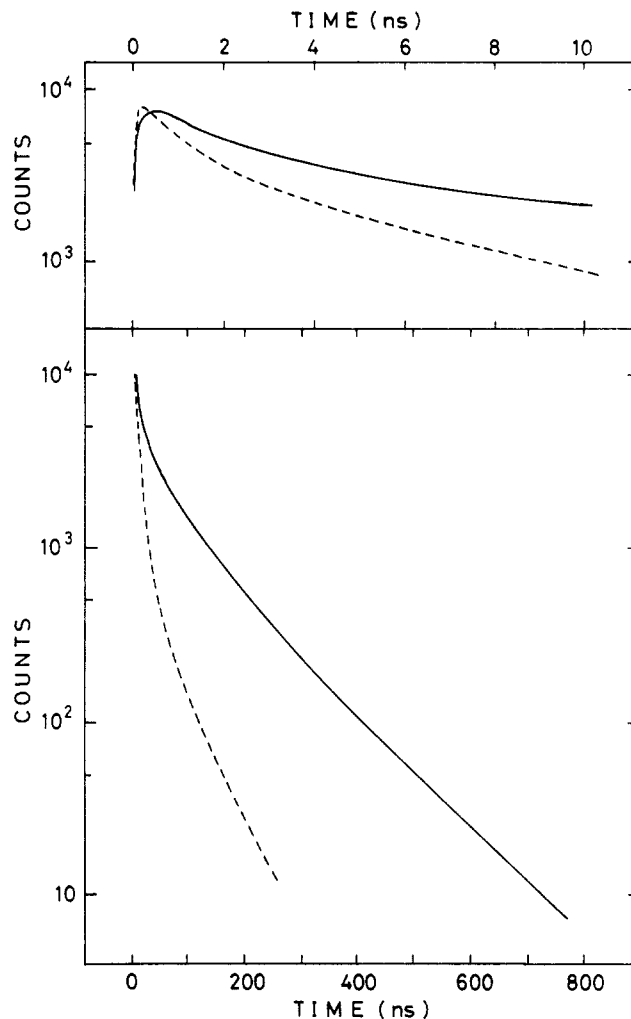


**Figure 8.** Fluorescence decay curves of the excimer  $E_1$  (---) and  $E_2$  (—) in the LB films, obtained from analyses of the time-resolved fluorescence spectra.

eq 2 by using the  $\gamma_A$  values obtained from the decay curve analysis (Table III). The value of the critical transfer distance  $R_0$  was taken from the value for the pyrene (donor)–pyrene (acceptor) pair which is known to be 10.03 Å.<sup>23</sup> The  $n_A$  values thus obtained are listed in Table III. It is seen that  $n_A$  has no linear relationship with the PHA concentration;  $n_A$  is increased only 1.6-fold with increasing PHA concentration from 0.8 to 28.6 mol %. On the other hand, the  $n_A$  value can be estimated from a computer simulation. We have recently calculated the densities of isolated monomers and aggregated species in the LB monolayer film. A model calculation was carried out by using a  $100 \times 100$  square lattice corresponding to an array of stearic acid molecules in the LB monolayer film.<sup>24</sup> The model patterns representing the distribution of PHA molecules were obtained by computer calculation that PHA molecules occupy lattice sites at random with its number corresponding to the PHA concentration. The number densities of isolated monomer, dimer, and higher aggregates were counted on 50 patterns for each PHA concentration. Finally, we obtained the average number densities of each species as a function of PHA concentration. The results are compared in Table III with the experimental values. In this table, calculated values are listed for the total number density of dimers and higher aggregates as energy traps. At a high concentration of PHA (28.6 mol %), the calculated values of  $n_A$  are close to the experimental values. On decreasing the PHA concentration, the calculated value is

(18) Hauser, M.; Klein, U. K. A.; Gosele, U. *Z. Phys. Chem. (Frankfurt am Main)* **1976**, *101*, S255.

(19) Kemnitz, K.; Murao, T.; Yamazaki, I.; Nakashima, N.; Yoshihara, K. *Chem. Phys. Lett.* **1983**, *101*, 337.

(20) Kemnitz, K.; Tamai, N.; Yamazaki, I.; Nakashima, N.; Yoshihara, K. *J. Phys. Chem.* **1986**, *90*, 5094.

(21) Anfinrud, P.; Crackel, R. L.; Struve, W. S. *J. Phys. Chem.* **1984**, *88*, 5873.

(22) Tamai, N.; Yamazaki, T.; Yamazaki, I. *J. Phys. Chem.* **1987**, *91*, 841.

(23) Berlman, I. B. *Energy Transfer Parameters of Aromatic Compounds*; Academic: New York, 1973.

(24) Yamazaki, I.; Tamai, N.; Yamazaki, T. In *Ultrafast Phenomena V*, Springer Series on Chemistry and Physics; Fleming, G. R., Siegman, A. E., Eds.; Springer-Verlag: Berlin, 1986; Vol. 46, pp 444–446.

significantly smaller than the experimental value. In other words, the effective trap density is far higher than expected, especially at lower concentrations of PHA. Such an experimental result can be interpreted only if a nonuniform distribution of PHA molecule is assumed in the LB film. In conformity with the foregoing discussion on the kinetic equation, the mixed LB monolayer film has an island structure due to aggregation of guest molecules. It is probable that, when the mixture of stearic acid and PHA molecules dissolved in benzene solution are spread on the water surface, PHA molecules form aggregates owing to the diffusion of PHA in a stearic acid monolayer before compression. Such an effect may be more pronounced at lower PHA concentrations than at higher concentrations.

**Rise and Decay Curves of Excimer Fluorescence  $E_2$  and  $E_1$ .** Fluorescence rise and decay curves of the excimer band  $E_2$  and  $E_1$  are shown in Figure 8, which were obtained from plots of the fluorescence intensities of the respective components in the time-resolved spectra (Figure 4). In the fluorescence rise curve of  $E_2$ , a delay can be seen after excitation. The decay curve analysis based on multiexponential decay kinetics shows a rise with a 150-ps time constant and two exponential decays with lifetimes of 5.5 and 28.4 ns. The 150-ps rise might be associated with the fastest decay of the dimer fluorescence D (170 ps). This is direct evidence for the assignment that excimer  $E_2$  forms from the ground-state dimer D. On the other hand, the rise time of the  $E_1$  excimer fluorescence is extremely short in comparison with  $E_2$  and is comparable to the rise of the excitation pulse. The decay of  $E_1$  is also faster than that of  $E_2$ . These facts correspond to the assignment that the  $E_1$  excimer originates from weak molecular interactions as discussed below. The decay curves of both  $E_1$  and  $E_2$  are not single exponential, and may be interpreted in terms of energy trapping by some higher aggregated species. Further detailed analyses along this line are now in progress.

**Excimer Conformation of  $E_1$ .** The spectroscopic features of the  $E_1$  fluorescence emission are summarized as follows: (1) The spectral band profile is broad and structureless, similar to that of  $E_2$ , (2) the band position (420 nm) is significantly blue-shifted relative to that of  $E_2$  (470 nm), and (3) this band appears only in the initial time region (100 ps–10 ns) after a 10-ps pulsed excitation; it rises much faster and decays much more rapidly than that of  $E_2$ , and that the time behavior is seemingly constant irrespective of the PHA concentration. We assign this band  $E_1$  as originating from an excimer with a conformation different from the ordinary sandwich excimer ( $E_2$ ). In this connection, recent works on the molecular association of pyrene chromophores in a vapor-deposited film of 12-(1-pyrenyl)dodecanoic acid<sup>25,26</sup> are worthy of notice. In a vapor-deposited film having a layered structure similar to the Y-type LB film concerned in the present study, the time-resolved fluorescence spectra show a broad fluorescence band at 420 nm apart from the well-known excimer band at 470 nm. Furthermore, recent studies of the time-resolved

fluorescence spectroscopy of pyrene in neat liquid<sup>27</sup> and in single crystal<sup>28</sup> show also a similar fluorescence band at 420 nm, although they gave no detailed discussion about the assignment of this band. The appearance of this broad band at 420 nm can be recognized as an emission band inherent of pyrene in molecular assemblies.

Several examples have been known concerning excimer formation with different conformations. Poly(*N*-vinylcarbazole) in solutions<sup>2,29,30</sup> and in amorphous films<sup>31</sup> emits two distinct fluorescence bands from different types of excimers; one is a broad band at 420 nm assigned to a singlet excimer with a sandwich-type structure of neighboring carbazole rings, and the other is a broad band at 380 nm assigned to fluorescence from a more weakly bound singlet excimer. The latter excimer, which was first observed by Johnson and Offen,<sup>29</sup> is called the second excimer. Itaya et al.<sup>30</sup> have supposed it to originate from two neighboring carbazole chromophores mutually overlapping one benzene ring in the excited state. Subsequently, De Schryver et al.<sup>2</sup> confirmed its conformation by using the racemic dimer model compounds. On the other hand, Matsui et al.<sup>32,33</sup> have demonstrated that the  $\beta$ -perylene crystal shows two distinct fluorescence bands due to two types of self-trapped excitons at 485 and 520 nm. They assigned these two bands as originating from different conformations of excited perylene molecules in the crystal; one is a two-center, sandwich-type conformation, and the other is a one-center type. In the latter case, the photoexcited molecule interacts with several molecules situated around the excited molecules. This is in striking contrast with the sandwich-type conformation where two molecules of excited and unexcited type interact. By reference to the above two cases, the excimer conformation of  $E_1$  would be a two-center or a one-center type. A thermodynamical study will be needed to get an insight into the excimer conformation in addition to a time-resolved fluorescence study.

The present study has been focused on excimer formation and fluorescence rise and decay kinetics in a LB monolayer film. The results are summarized as follows: (1) pyrene chromophores in LB films form two kinds of domain, i.e., an isolated monomer and a dimer and/or higher aggregate, with their respective densities depending on the PHA concentration; (2) in the aggregated domain, two types of excimers, i.e., a two-center sandwich type and a one-center or partial overlapping type, are formed within 200 ps after excitation; and (3) in the monomer domain, direct energy transfer and quenching is the dominant pathway for the energy relaxation process.

**Registry No.** PHA, 90936-84-8; pyrene, 129-00-0; stearic acid, 57-11-4.

(25) Mitsuya, M.; Taniguchi, Y.; Tamai, N.; Yamazaki, I.; Masuhara, H. *Thin Solid Films* **1985**, *129*, L45.

(26) Taniguchi, Y.; Mitsuya, M.; Tamai, N.; Yamazaki, I.; Masuhara, H. *Chem. Phys. Lett.* **1986**, *132*, 516.

(27) Horiguchi, R.; Iwasaki, N.; Maruyama, Y. *J. Phys. Chem.*, in press.

(28) Matsui, A.; Mizuno, K.; Tamai, N.; Yamazaki, I. *Chem. Phys.* **1987**, *113*, 111.

(29) Johnson, P. C.; Offen, H. W. *J. Chem. Phys.* **1971**, *55*, 2945.

(30) Itaya, A.; Okamoto, K.; Kusabayashi, S. *Bull. Chem. Soc. Jpn.* **1976**, *49*, 2082.

(31) Nozue, Y.; Hisamune, T.; Goto, T.; Tsuruta, H. *J. Phys. Soc. Jpn.* **1983**, *52*, 2983.

(32) Matsui, A.; Mizuno, K.; Nishimura, H. *J. Phys. Soc. Jpn.* **1984**, *53*, 2818.

(33) Nishimura, H.; Yamaoka, T.; Mizuno, K.; Iemura, M.; Matsui, A. *J. Phys. Chem. Soc. Jpn.* **1984**, *53*, 3999.